CIMSA 2005 – IEEE International Conference on
Computational Intelligence for Measurement Systems and Applications
Giardini Naxos, Italy, 20-22 July 2005

Automatic Morphological Analysis for Acute Leukemia Identification in Peripheral Blood Microscope Images

Fabio Scotti
University of Milan, Department of Information Technologies, via Bramante 65, 26013 Crema, Italy

Abstract – *The early identification of acute lymphoblastic leukemia symptoms in patients can greatly increase the probability of recovery. Nowadays the leukemia disease can be identified by automatic specific tests such as Cytogenetics and Immunophenotyping and morphological cell classification made by experienced operators observing blood/marrow microscope images. Those methods are not included into large screening programs and are applied only when typical symptoms appears in normal blood analysis. The Cytogenetics and Immunophenotyping diagnostic methods are currently preferred for their great accuracy with respect to the method of blood cell observation which presents undesirable drawbacks: slowness and it presents a not standardized accuracy since it depends on the operator's capabilities and tiredness. Conversely, the morphological analysis just requires an image -not a blood sample- and hence is suitable for low-cost and remote diagnostic systems. The presented paper shows the effectiveness of an automatic morphological method to identify the Acute Lymphocytic Leukemia by peripheral blood microscope images. The proposed system firstly individuates in the blood image the leucocytes from the others blood cells, then it selects the lymphocyte cells (the ones interested by acute leukemia), it evaluates morphological indexes from those cells and finally it classifies the presence of the leukemia.*

Keywords *– Automatic Leukemia Identification, Acute Leukaemia, Morphological Analysis, Blast Cells, Lymphoblast, Leucocytes analysis.*

I. INTRODUCTION

Acute Lymphocytic Leukemia (ALL), also known as acute *lymphoblastic* leukemia is a cancer of the white blood cells, characterized by the overproduction and continuous multiplication of malignant and immature white blood cells (referred to as *lymphoblasts* or *blasts*) in the bone marrow. It is fatal if left untreated due to its rapid spread into the bloodstream and other vital organs. ALL produces a lack of healthy blood cells due to an abnormal number of malignant and immature white blood cells [1]. It mainly affects young children and adults over 50. Early diagnosis of the disease is fundamental for the recovery of patients especially in the case of children.

Unfortunately, the initial symptoms of ALL are quite aspecific: generalized weakness, anemia, frequent fever and infections, weight loss and/or loss of appetite, excessive bruising or bleeding from wounds, nosebleeds, bone pain, joint pains, breathlessness, enlarged lymph nodes, liver and/or spleen. If the described symptoms are present, blood tests such as a full blood count, renal function, electrolytes and liver enzymes and blood count have to be done. Clinical suspicion alone may be the only reason to perform a bone marrow biopsy, which is the next step in the diagnostic process. Bone marrow is examined for blasts, cell counts and other signs of disease. Pathological examination [2], cytogenetics [3] and immunophenotyping are common diagnostic analysis. Once the blast-cells invasion starts, blast cells can be detected into the peripheral blood.

Figure 1 shows the microscope image of a blood film (left) and it plots three examples of normal lymphocytes and three lymphoblasts cells (right). Images in Figure 1 have been digitalized by the optical microscope by usgin a CCD and then acquired by a frame-grabber system [4]. Principal cells present in the blood are the *red* blood cells, and the *white* cells (leucocytes). Leucocyte cells containing granules are called granulocytes (composed by *neutrophil*, *basophil*, *eosinophil*). Cells without granules are called agranulocytes (*lymphocyte* and *monocyte*) [1]. ALL symptoms are associated only to the lymphocytes.

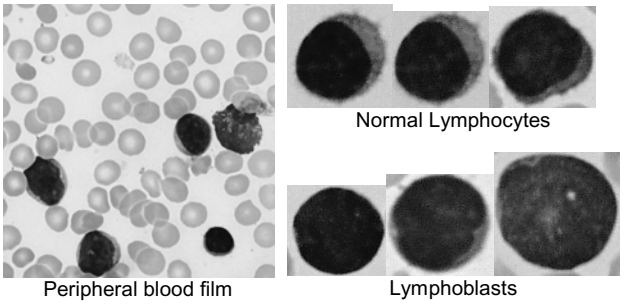

Figure. 1. Peripheral blood film (left) with white cells marked with colorant. On the right, examples of normal (top) and blast (down) lymphocytes acquired with 1000x microscope.

Hence, the observation of the peripheral blood film by expert operators is *one* of the diagnostic procedures available to evaluate the presence of the acute leukemia. This analysis suffers from slowness and it presents a not standardized accuracy since it depends on the operator's capabilities and tiredness. Conversely, the morphological analysis just requires an image -not a blood sample- and hence is suitable for low-cost, standard-accurate, and remote diagnostic systems.

Our work aims to demonstrate that the peripheral blood film observation can be fully automated and can be performed as ancillary/backup service to the physician

activity. In this framework, tens of thousand cells belonging to a blood slide can be analyzed looking for one blast cell. Only few attempts of partial/full automated systems based on image-processing systems are present in literature and they are still at prototype stage [5, 6].

The system we propose firstly individuates in the blood image the leucocytes from the others blood cells, then it extracts the lymphocyte cells (the ones interested by acute leukemia), it extracts morphological indexes from those cells and finally it classifies the presence of the leukemia using neural networks. The overall system is described in section 2. Section 3 focuses on how to extract a suitable set of morphological indexes from the leucocytes in order to identify the blast cells by a classifier. Section 4 describes the design of the classifier, how classification accuracy can be tested and how a proper classifier can be chosen from a set of candidates of different families of classifiers.

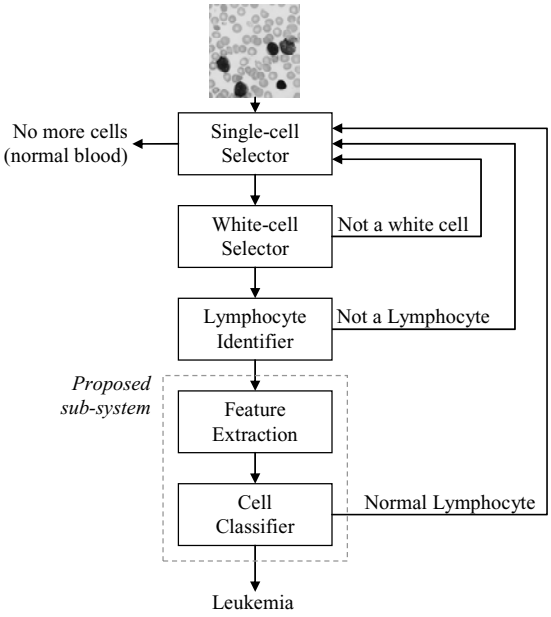

Figure 2. The structure of modules composing the acute leukemia classification system.

II. THE IMAGE PROCESSING SYSTEM

The main modules which compose the overall system are plotted in Figure 2. The *Single-cell Selector* module firstly enhances the input image and identifies the single cells. It has been composed by adaptive prefiltering and segmentation algorithms. Secondly, the *White-cells Identifier* module selects the white cells present into the image by separating them from others blood's components (red cells and platelets). The third module (the *Lymphocyte Identifier*) can recognize a lymphocyte with respect to the other selected white cells. A complete description of these three modules has been given in [7]. The three presented modules can recognize leucocytes in a blood film image with a mean error of about 0.02%. Typically, the main source of error is related to the strong morphological similarities between the components of the leucocytes family (lymphocytes, monocytes, etc.), conversely is much less probable to classify the other blood components (such as red cells) as lymphocyte than vice versa [7]. In general, the first three modules of the system in Figure 2 can select sub-images of lymphocytes from the blood film image with high accuracy. Examples of sub-images containing a lymphocyte produced by the described chain are given in Figure 1 (the sub-images on the left).

The system we propose in this paper is the sub-system which has to recognize if a lymphocyte is blast or normal, and it is composed by the modules inside the dashed line in Figure 2: the *Feature Extraction* module and the *Classification* module. The Feature Extraction module processes a sub-image containing a lymphocyte coming from the Lymphocyte Identifier module and it produces in output a set of morphological indexes. The classification module processes those indexes in order to classify the cell as blast or normal. If the system finds a blast cell, the *blast cell counter* is increased; otherwise a new lymphocyte will be processed. The two modules perform the *automatic morphological analysis* of lymphocyte images.

III. AUTOMATIC MORPHOLOGICAL ANALYSIS

The classification of the lymphocyte sub-image is quite complicated since even an expert operator can have dubs in classifying some lymphocyte cells. Actually, the morphological distinctive aspects of blast and normal lymphocytes are very smooth.

The features we want to extract from the cell are mostly the features that the operators qualitatively observe in the blood film to classify the cell as blast or normal. The most common leukemia classification is the FAB method [8]; nowadays it has been updated with the immunologic classification [3] which it is not image-based. Otherwise, the FAB method is still valid for image-based morphological classification. Concerning the ALL, the FAB classification is three-partitioned as follow:

- ***L1***: Blasts are small and homogeneous. The nuclei are round and regular with little clefting and inconspicuous nucleoli. Cytoplasm is scanty and usually without vacuoles.
- ***L2***: blasts are large and heterogeneous. The nuclei are irregular and often clefted. One or more, usually large nucleoli are present. The volume of cytoplasm is variable, but often abundant and may contain vacuoles.
- ***L3***: blasts are moderate-large in size and homogeneous. The nuclei are regular and round-oval in shape. One or more prominent nucleoli are present. The volume of cytoplasm is moderate and contains prominent vacuoles.

Figure 3 shows the great variability in shape and pattern of the blast cells according to the FAB classification.

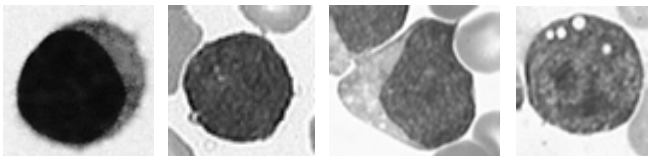

Figure 3. Morphological variability associated to the blast cells according to the FAB classification.

Our goal is to detect without differentiation the presence of all three types of blasts in the blood film. The goal is achieved by a sequence of phases which as been schematized in Figure 4. Once the previously described chain separates each lymphocyte in a sub-image, the proposed system extracts the morphological indexes in three subsequent steps: firstly processing the *membrane*, then the *cytoplasm* and finally the *nucleus*. All processed indexes are in input to the classifier system which performs the classification.

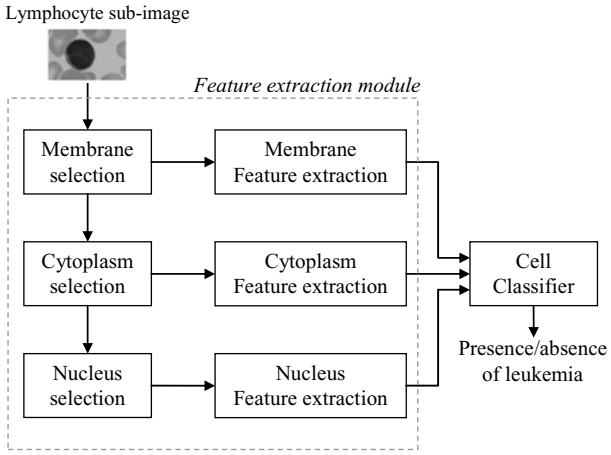

Figure 4. Structure of the feature extraction module and the classifier module.

A. Lymphocyte membrane selection

Let us now discuss each step composing the *membrane selection* phase of the external membrane. Figure 5 shows the main steps and examples of input/output images:

#1. *Sobel edge enhancing*. This step enhances the borders of the membranes [9] in order to better perform the subsequent edge detection steps. An edge-enhanced gray-level image is hence produced. This processing step is recommended since it helps to better segment grouped cells (i.e., the second and third input images in Figure 5).

#2. *Adaptive Canny edge detection*. This step reconstructs the borders of the membranes. Canny-based filters [10] have to be preferred for their intrinsic capacity to ensure in output a continuous edge. The output of this step is a binarized image (third row in Figure 5). The standard deviation of the Gaussian filter used in the Canny operator has been adapted to 1/15 of the measured average cell diameter **D**. Experiments show that this value allows the filters to "match" the estimated membrane thickness. A complete description of the estimation of the average cell diameter is available in [7].

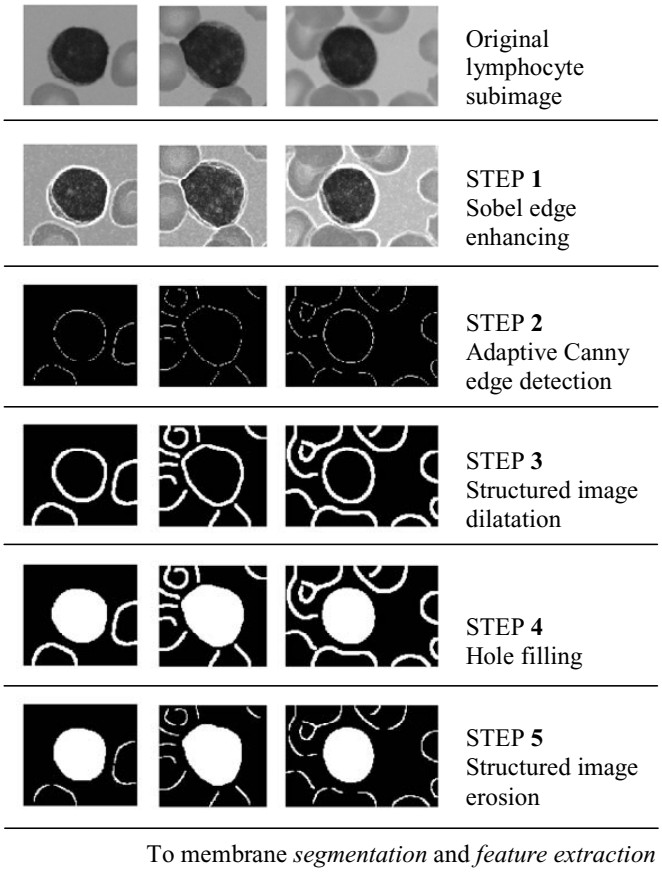

Figure 5. From the lymphocyte gray-level sub-image, to the selection of the external membrane. Examples of isolated (first column) and grouped lymphocytes (second and third column) are plot.

#3. *Structured image dilation.* The morphological operator called dilation [10] has been used to better connect separated points of the membrane border and to make the perimeter of the cell as a connected item (thicker more than one pixel) as shown in the fourth row in Figure 5. Again, the structured element used by the dilatation operator has been adapted to 1/15 **D**.

#4. *Hole filling*. This step consists of filling internal holes of the connected element with biggest area in the processed image [10,11]. The biggest connected element in the region of interest is indeed the membrane perimeter (fifth row in Figure 5). This hypothesis is reasonable since the red cells are mostly smaller than the lymphocytes and with an evident "hole" in the center.

#5. *Structured image erosion*. This step applies to the binary image in input an erosion morphological filter with a structuring element composed by a square 2x2 matrix. This step reduces the spur elements that can be left along the membrane edges. The usage is more related to

visualization aspects. Experiments showed that it can be considered as optional since it not produces appreciable increments in the classifier's accuracy.

The correctness of previously performed steps can be controlled: we expect a cell perimeter slightly around the value $\pi\mathbf{D}$. In our analysis we consider as correct the values of the perimeter that ranges between 0.95-2.5 of $\pi\mathbf{D}$. If the perimeter value is out of the range, wrong membrane detection can be occurred. In this case, the processed sub-image is discarded. That avoids further errors in the feature extraction phase or classification errors. If the perimeter value is in the fixed range, the algorithm segments the processed image, it selects the connected element with the biggest area and it crops from the original image the selected lymphocyte (Figure 6).

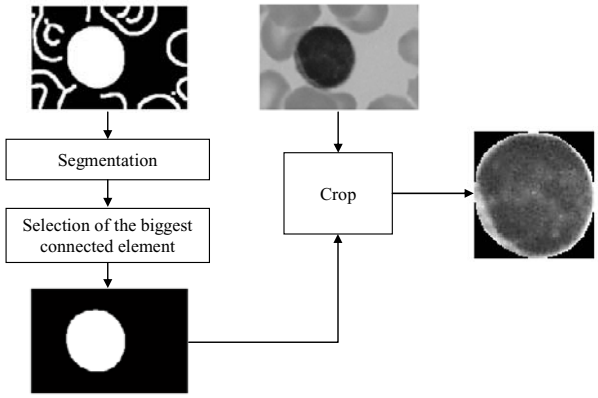

Figure 6. Selection of the lymphocyte cell.

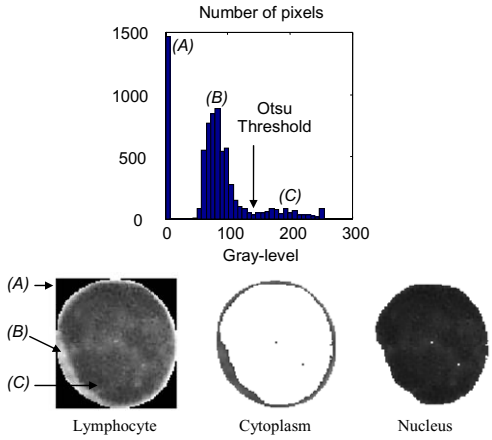

Figure 7. Lymphocyte histogram analysis for nucleus and cytoplasm selection.

B. Nucleus and Cytoplasm selection

The phase of *nucleus* and *cytoplasm selection* exploits the cell image resulted from the previous step (Figure 6). The selection of the two inner areas of the cell that correspond to the nucleus and cytoplasm can be done by a thresholded segmentation. That arises from the fact that the cytoplasm and the nucleus are almost uniform areas with respect to the gray level intensity.

In this situation the gray level histogram of cells tends to be bimodal. Figure 7 shows a typical lymphocyte cell extracted from the blood film by using the described processing chain (on the right) and its histogram. The principal components of the histogram are shown with capital letters. The *(A)* peak can be discarded since it comes from the lateral zero-valued pixels outside the cropped areas in the rectangular image. The peaks *(B)* and *(C)* come from the nucleus and cytoplasm areas respectively. The difference in height of the peaks is typical since the area of the cytoplasm is lower than the area of the nucleus.

The threshold level used to segment the nucleus from the cytoplasm in the cell image can be found as the threshold that better separates the two distributions B and C of gray level in the histogram. In the literature many techniques are available [9,10]. In this paper we used the Otsu's method [12] for its absence of assumptions of the models generating the distributions on the image. The method simply chooses the gray-level threshold to minimize the intra-class variance of the thresholded black and white pixels. Experiments showed a good performance of this method in separating the nucleus from the cytoplasm. Figure 7 shows the result of the segmentation for a lymphocyte image.

Also in this phase it is possible to control the exactness of the selection procedure by controlling the area's value of the extracted nucleus. As a matter of fact, the nucleus' area must have a value smaller than the area of the external membrane. In addition, we evaluated that the value must be above a fixed threshold (50% of the membrane area in our study) since we assume that a classifiable lymphocyte must have a considerable nucleus. Otherwise the cell can be squeezed during the preparation of the film and, of course, it should be discarded from subsequent analysis.

C. Features extraction

Previous steps produced from the selected image of the lymphocyte six sub-images:

- three images containing portions of the original gray-level image (i.e., at the bottom of Figure 7);
- three black-and-white sub-images which represent only the borders of the membrane (i.e., at the bottom in Figure 6), the cytoplasm and the nucleus.

The first three sub-images can be used to extract features regarding the gray-level intensity pattern of the image (i.e., granularity of the color, uniformity). From the three black-and-white sub-images we can easily measure morphological features such as the perimeter, the area, the momentums of the image, etc.

At this stage, the extracted features from the sub-images will be used by the classifier to identify the presence of the ALL. The choice of the features has been driven by

suggestions of hematopathologist present in the literature [3,5]. In fact, experts classify cells by qualitatively evaluating the same cells properties. From the 3 black-and-white images the system processes the membrane parameters such as Area, Perimeter, Convex Area, Solidity, Major Axis Length, Orientation, Filled Area and Eccentricity defined as standard procedures present in the Matlab Image Processing Toolbox [10]. In addition we processed the ratio between the cell and nucleus areas, the nucleus' "*rectangularity*" (the ratio between the perimeter of the tightest bounding rectangle and the nucleus perimeter), the cell "*circularity*" (the ratio between the perimeter of the tightest bounding circle and the cell perimeter). From the three gray-level sub-images we extracted the mean gray-level value and its standard deviation in order to represent the variation of the intensity in the nucleus. Total number of extracted features is 23.

IV. EXPERIMENTAL RESULTS

The proposed system has been tested using sample-images extracted from an image repository provided by the M. Tettamanti Research Center for Childhood Leukemias and Hematological Diseases, Monza, Italy. The dataset consists of 113 images and it globally contains about 8400 blood cells, 150 of them are lymphocytes labeled by expert oncologists as normal or blast.

Our goal was to create the final classifier and test the subsystem proposed in this paper. For this reason we prepare 150 sub-images containing the lymphocytes, simulating the functioning of the previous modules of the overall systems. This operation allows to create a *human-classified* training dataset for the classifier that we want to design. The system has been tested in two phases.

A. Testing the selection modules

In the first test phase we tested the first three modules of the subsystem: the *membrane* selection module, the *cytoplasm* selection module and the *nucleus* selection module. In particular, those modules (Figure 4, left column of modules) correspond to the steps described in section III, and their accuracy is related to the concept of *correct selection*.

The case of *correct selection* is not easily definable by automatic procedures since we deal with images that are not synthetic but real. For this reason, we checked the areas selected by the modules by one-by-one manual observation. We consider a membrane and a nucleus of a lymphocyte as *correct-selected* if their membranes are correctly contained into the selected areas processed by the selection algorithms.

The free parameters of the proposed chain in section III (the dimensions of the structuring elements for morphological filters defined in step #3 and #5) were empirically set by trials on the dataset. As a result, the selection modules described in section III achieved correctly the selection task in 148 sub-images out of 150.

Figure 8 compares the two cases of not-correct selection compared to a case where correct selection occurred. It can be seen that the problem is related to the presence of compact stacks of cells around the lymphocyte. In this situation, the membrane thickness is very thin, and the algorithms can not correctly segment the areas. Notably, it does not happen in red-cell/lymphocyte adherences, but only in two cases of adherences between two lymphocytes. That is related to the fact that, in the case of adherences between lymphocytes, the differences in contrast between the two cells are much less than in the case of red-cell/lymphocyte adherences. The latter case is much more probable than the former because the percentage of red cells in the blood film is higher than lymphocytes.

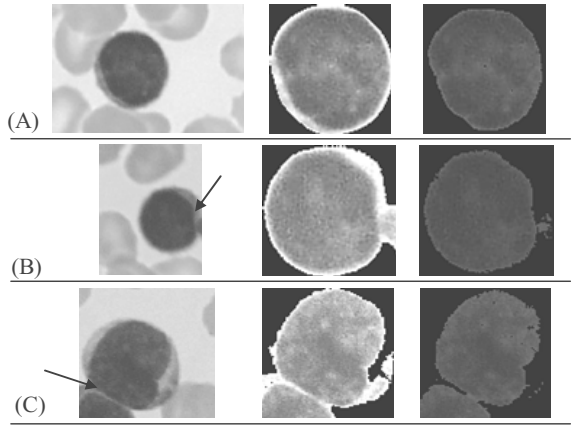

Figure 8. Correct (A) and wrong membrane selection (B,C). Arrows point at membrane adherences between lymphocytes.

B. Creating and testing the classifier

In the second test phase we created and validated the final module of the system: the classifier. Hence, we processed the 150 sub-images present into the dataset obtaining the features described in the previous section. As reported, it occurred two cases of wrong membrane selection and the related features that have been extracted suffer from errors: for example the nucleus area is overestimated (Figure 8, last row). The capability of the selected features in separating the normal lymphocyte from the blasts can be qualitatively evaluated by plotting the classes with respect to the three most relevant features: cell area, nucleus area and gray intensity of the cytoplasm (Figure 9). The most relevant features have been found by applying a feature selection technique called *forward selection* based on nearest neighbor classifier evaluated with Leave One Out method [13].

The evaluation of the system accuracy has been performed by N-fold cross-validation technique [13] where N was chosen equals to 10. The first classifier family we considered is the nearest neighbor classifiers (kNN). Different kNN classifiers have been created ranging the number of nearest neighbors k from 1 to 15 and considering the Euclidean,

cubic and Manhattan norm [13]. Feed-forward neural networks with log-sigmoidal activation function (FF-NN) and with two hidden layers have been created by ranging the number of the hidden units from 2 to 50. We used the Back-propagation method present in the Matlab Neural Network Toolbox [10]. Also a linear Bayes Normal classifier [13] has been used as reference using the routines available in the well-known Matlab toolbox for pattern recognition *PRTool* [14].

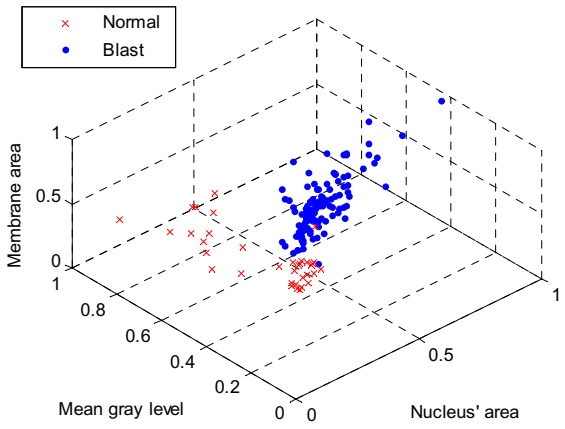

Figure 9. Separation of classes using the three most relevant features: cell and nucleus normalized area and relative gray intensity of nucleus.

TABLE 1. Accuracy of the best classifiers (23 features).

Type	Mean error	Standard deviation	Execution time	Note
LINEAR	0.040	0.0344	601 µs	Bayes normal classifier
KNN	0.0267	0.0344	1254 µs	K=1 Euclidean norm
FF-NN	0.0133	0.0281	1001 µs	[20,1] Neurons

Table 1 reports the results of the best classifier for each family that as been found during the validation test (on a Intel Centrino 1,4Ghz, Windows XP, 750 Mb Ram, Matlab 7, PRTools, version 4.0.13). Notably the feed-forward neural network with 20 hidden neurons achieves the lowest mean miss-classification error (with lowest standard deviation). Interestingly, the corresponding processing time is not the highest with respect to other tested classifiers. That is satisfactory since the final systems must be built exploiting enlarged dataset. In fact, the computation complexity of the kNN classifier is almost proportional to the training dataset size. On the contrary feed-forward neural networks' complexity is related to the number of neurons which tends to be much lower than the number of training samples.

Results show that the automatic classification of Acute Lymphocytic Leukemia starting from lymphocyte images is possible and accurate. Authors believe that the usage of inductive classifier (i.e., feed-forward neural networks) is very suited to the application and higher accuracy can be achieved when the number of sample images will be increased.

V. CONCLUSIONS

This paper presented a methodology to achieve a fully automated classification of the Acute Lymphocytic Leukemia from microscope blood-film images. The methodology is based on the morphological analysis of blood's white cells (lypmphocyes). Results show that the presented methodology is achievable and it offers remarkable classification accuracy. Further studies will be focused on enhanced adaptive segmentation modules, the impact on classification accuracy of enlarged sample dataset and the test of the overall system.

ACKNOWLEDGMENTS

I wish to thanks prof. Andrea Biondi and Dr. Oscar Maglia from M. Tettamanti Research Center for Childhood Leukemias and Hematological Diseases -Monza, Italy- for their profitable cooperation and encouragement, the data provided and the careful classification of sample images.

REFERENCE

[1] K. Breden, T. Schorr, J. B. Schorr, "Blood" Colliers Encyclopaedia, Vol. 4, 1978
[2] Abbott Diagnostics Website, http://www.abbott.com/products/diagnostics.htm/
[3] A. Biondi, G. Cimino, R. Pieters, C. H. Pui, "Biological and therapeutic aspects of infant leukemia", Blood, Vol. 96, No. 1, pp. 24-33, July, 2000
[4] F. Cillesen, W. Der Meer, "Atlas of Blood Cell Differentiation", Elsevier Science B.V., Amsterdam, The Netherlands, 1998
[5] D.S. Serbouti et al., "Image segmentation and classification methods to detect leukemias", Annual international conference of IEEE engineering in Medicine and Biology society, Vol.13, No.1, 1991
[6] Dj. Foran, et al. "Computer-assisted discrimination among malignant lymphomas and leukemia using immunophenotyping, intelligent image repositories, and telemicroscopy", IEEE Trans. Inf. Technol. Biomed., pp. 265-73, December 2000
[7] V. Piuri, F. Scotti: "Morphological Classification of Blood Leucocytes by Microscope Images" Proc. International Symposium on Computational Intelligence for Measurement Systems and Applications, Boston, MD, USA, July 2004
[8] J.M. Bennett et al. "Proposals for the classification of the acute leukaemias. French-American-British (FAB) co-operative group", Br J Haematol.; Vol. 4, No. 33, pp. 451-458, August, 1976
[9] J.S. Lim "Two dimensional signal and image processing" Prentice Hall 1990
[10] R. C. Gonzalez, R. E. Woods, S.L. Eddins, "Digital Image Processing Using MATLAB", Pearson Prentice Hall Pearson Education, Inc., New Jersey, USA, 2004
[11] H. J. A. M. Heijmans (1994): Morphological Image Operators, Academic Press, New York
[12] N. Otsu, "A Threshold Selection Method from Gray-Level Histograms" IEEE Transactions on Systems, Man, and Cybernetics, Vol. 9, No. 1, pp. 62-66, 1979
[13] A.K. Jain, R.P.W. Duin, and J. Mao, "Statistical pattern recognition: A review," IEEE Transactions on Pattern Analysis and Machine Intelligence, Vol. 22, No. 1, pp. 4-37, 2000
[14] F. van der Heiden, R.P.W. Duin, D. de Ridder, and D.M.J. Tax, Classification, Parameter Estimation, State Estimation: An Engineering Approach Using MatLab, Wiley, New York, 2004